Calculation of antenna radiation center using angular momentum

Fridén, Jonas; Kristensson, Gerhard

Published in:
7th European Conference on Antennas and Propagation (EuCAP), 2013

2013

Calculation of antenna radiation center using angular momentum

Jonas Fridén*, Gerhard Kristensson†

*Ericsson Research
Ericsson AB
Lindholmspiren 11, 417 56 Göteborg, Sweden
Email: jonas.friden@ericsson.com
†Department of Electrical and Information Technology
Lund University
P.O. Box 118, SE-221 00 Lund, Sweden
Email: gerhard.kristensson@eit.lth.se

***Abstract*—An algorithm to compute the radiation center of an antenna based on the Spherical wave expansion (SWE) is presented. The method is based on the angular momentum vector quantity that is uniquely defined for any antenna far field pattern. The radiation center is defined as the unique point where the magnitude of the angular momentum is minimized with respect to active translations of the far field. This corresponds to minimizing the phase variations in the antenna far field pattern. In addition, the current distribution axis can be determined, corresponding to minimization of the vertical component of angular momentum with respect to rotations.**

***Index Terms*—radiation center; phase center; antenna orientation; angular momentum; spherical wave expansion**

I. Introduction

The far field amplitude $\boldsymbol{F}(\hat{\boldsymbol{r}})$ is defined as the limit

$$\boldsymbol{F}(\hat{\boldsymbol{r}}) = \lim_{r\to\infty} \sqrt{\frac{4\pi}{\eta_0}} r e^{jkr} \boldsymbol{E}(\boldsymbol{r}) \tag{1}$$

with an underlying time convention $\exp(\mathrm{j}\omega t)$, vaccuum impedance $\eta_0 = \sqrt{\mu_0/\epsilon_0}$, and $k = 2\pi/\lambda$.

The Spherical wave expansion (SWE) of the far field amplitude $\boldsymbol{F}(\hat{\boldsymbol{r}})$ is

$$\boldsymbol{F}(\hat{\boldsymbol{r}}) = \sum_{\tau lm} a_{\tau lm} \boldsymbol{A}_{\tau lm}(\hat{\boldsymbol{r}}), \tag{2}$$

Here, the summation is over $\tau = 1, 2$ for electric and magnetic modes, $l = 1, 2, \ldots, \infty$, and $m = -l, \ldots, l$, see [1]. Using the orthonormal vector spherical harmonics $\boldsymbol{A}_{\tau lm}$, implies that

$$a_{\tau lm} = \iint_{\Omega} \boldsymbol{A}^*_{\tau lm}(\hat{\boldsymbol{r}}) \cdot \boldsymbol{F}(\hat{\boldsymbol{r}}) \mathrm{d}\Omega. \tag{3}$$

Here, Ω denotes the unit sphere, and $\mathrm{d}\Omega$ is the surface measure.

It is well known that truncation limits for SWEs depend on the physical size, position, and orientation of the antenna [1]. By using the relation between the vector spherical harmonics and the angular momentum, it is natural to quantify the mode contents in terms of angular momentum. The definitions are:

$$\begin{cases} L^2 = \displaystyle\sum_{\tau lm} l(l+1)|a_{\tau lm}|^2, \\ L_z^2 = \displaystyle\sum_{\tau lm} m^2 |a_{\tau lm}|^2. \end{cases} \tag{4}$$

where $a_{\tau lm}$ are the mode coefficients (3).

II. Method

Minimizing L^2 corresponds to finding the smallest sphere that circumscribes the antenna currents. This can be achieved by active translations of the far fields, and it leads to a lowering of the used l and m-indices. In this sense, the phase variations are minimized, and the origin of the minimum sphere is related to the phase center. The origin of the minimum sphere is denoted *radiation center* $\boldsymbol{d}_{\mathrm{RC}}$, see Fig. 1. Note that the IEEE definition of phase center [2] is slightly vague and only useful for antennas with manifest main lobes.

> "**2.270** phase center. The location of a point associated with an antenna such that, if it is taken as the center of a sphere whose radius extends into the far-field, the phase of a given field component over the surface of the radiation sphere is essentially constant, at least over that portion of the surface where the radiation is significant."

However, the proposed approach is applicable for any far field pattern. In fact, in [3] it is proven that the radiation center is unique for any far field pattern with radiated power $P_{\mathrm{rad}} > 0$.

In the same way, L_z^2 is minimized by finding the smallest cylinder that circumscribes the antenna currents. Hence, rotations can be used, and the symmetry axis of the minimum cylinder is by definition the *current distribution axis*.

Note that L^2 is invariant under rotations [1, 3]. This implies that the minimization of L^2 by translations can be performed first. Thereafter, a consecutive minimization of L_z^2 by rotations can be performed while keeping L^2 minimized.

978-88-907018-3-2/13

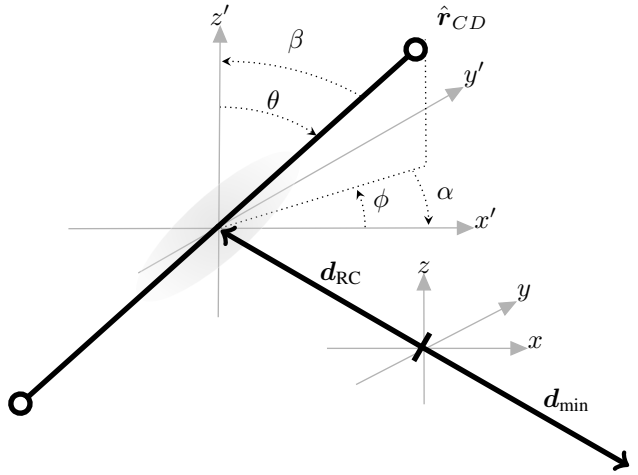

Fig. 1. The translation $\boldsymbol{d}_{\text{min}}$ that minimizes L^2 defines the *radiation center* $\boldsymbol{d}_{\text{RC}}$. A rotation, $\alpha = -\phi$ around the z-axis followed by $\beta = -\theta$ around the y axis, that minimizes L_z^2, defines the *current distribution axis* $\hat{\boldsymbol{r}}_{CD}$. The current distribution is depicted as a grey ellipsoid.

III. Results

The main results of this work is that the radiation center is a unique point in space for any antenna radiation pattern [3]. The only criterion is that the radiated power $P_{\text{rad}} > 0$. Moreover, an analytical method to quantify the uniqueness of the current distribution axis is also presented, in terms of investigation of the eigenvalues of a three-dimensional dyadic. The derivations of these results are obtained by defining L^2 and L_z^2 in terms of the angular momentum operator $\mathcal{L} = -j\boldsymbol{r} \times \nabla$ acting on the far field amplitude $\boldsymbol{F}(\hat{\boldsymbol{r}})$ [3]. Note that $\mathcal{L}$ is a measure of the variations perpendicular to $\boldsymbol{r}$, *i.e.*, the angular variations. By orthogonality and completeness of the vector spherical harmonics $\boldsymbol{A}_{\tau lm}$, the squared angular momentum operation can also be defined as

$$L^2 = \iint_\Omega \boldsymbol{F}^*(\hat{\boldsymbol{r}}) \cdot \mathcal{L}^2 \boldsymbol{F}(\hat{\boldsymbol{r}}) \mathrm{d}\Omega. \tag{5}$$

The explicit form of the $\mathcal{L}^2$ operator in spherical coordinates is

$$\mathcal{L}^2 = -\frac{1}{\sin\theta}\frac{\partial}{\partial\theta}\left(\sin\theta\frac{\partial}{\partial\theta}\right) - \frac{1}{\sin^2\theta}\frac{\partial^2}{\partial\phi^2} \tag{6}$$

Let $L^2(\boldsymbol{d})$ be L^2 for the antenna far field translated by the length vector $\boldsymbol{d}$, *i.e.*, the field

$$\boldsymbol{F}'(\hat{\boldsymbol{r}}) = \boldsymbol{F}(\hat{\boldsymbol{r}})\mathrm{e}^{\mathrm{j}k\hat{\boldsymbol{r}}\cdot\boldsymbol{d}}. \tag{7}$$

Applying (5) leads to the quadratic form

$$L^2(\boldsymbol{d}) = L^2(\boldsymbol{0}) - 2k\boldsymbol{a}_1 \cdot \boldsymbol{d} + k^2 \boldsymbol{d} \cdot \mathbf{A}_2 \cdot \boldsymbol{d}. \tag{8}$$

with coefficients [3]

$$\begin{cases} a_0 = L^2(\boldsymbol{F}(\hat{\boldsymbol{r}}), \boldsymbol{0}) = \iint_\Omega \boldsymbol{F}^*(\hat{\boldsymbol{r}}) \cdot \mathcal{L}^2 \boldsymbol{F}(\hat{\boldsymbol{r}}) \mathrm{d}\Omega, \\ \boldsymbol{a}_1 = \iint_\Omega \mathrm{Im}\left[F_\theta \nabla_\Omega F_\theta^* + F_\phi \nabla_\Omega F_\phi^*\right] \mathrm{d}\Omega \\ \quad - 2\iint_\Omega \cot\theta \mathrm{Im}(F_\theta F_\phi^*)\hat{\boldsymbol{\phi}}\mathrm{d}\Omega, \\ \mathbf{A}_2 = \iint_\Omega \boldsymbol{F}^*(\hat{\boldsymbol{r}}) \cdot \boldsymbol{F}(\hat{\boldsymbol{r}})[\hat{\boldsymbol{\theta}}\hat{\boldsymbol{\theta}} + \hat{\boldsymbol{\phi}}\hat{\boldsymbol{\phi}}]\mathrm{d}\Omega. \end{cases} \tag{9}$$

Here, the transverse nabla operator

$$\nabla_\Omega = \hat{\boldsymbol{\theta}}\frac{\partial}{\partial\theta} + \hat{\boldsymbol{\phi}}\frac{1}{\sin\theta}\frac{\partial}{\partial\phi} \tag{10}$$

is used. Note that $\boldsymbol{a}_1$ is a real-valued vector. Moreover, $\mathbf{A}_2$ is a real-valued symmetric dyadic that is positive definite if

$$P_{\text{rad}} = \iint_\Omega \boldsymbol{F}^* \cdot \boldsymbol{F} \mathrm{d}\Omega > 0.$$

This guarantees a unique minimum at

$$\boldsymbol{d}_{\text{min}} = \mathbf{A}_2^{-1} \cdot \boldsymbol{a}_1 / k = -\boldsymbol{d}_{\text{RC}} \tag{11}$$

which implicitly defines the radiation center $\boldsymbol{d}_{\text{RC}}$, see Fig. 1.

A. Translation of the radiation center — additivity

Consider a far field $\boldsymbol{F}(\hat{\boldsymbol{r}})$ with a given radiation center. Hence, by (11)

$$\boldsymbol{a}_1(\boldsymbol{F}) = -k\mathbf{A}_2(\boldsymbol{F}) \cdot \boldsymbol{d}_{\text{RC}}.$$

Now consider the translated farfield $\boldsymbol{F}'$, see (7). To calculate $\boldsymbol{a}_1(\boldsymbol{F}')$ note that

$$\begin{aligned} &F_\theta \mathrm{e}^{\mathrm{j}k\hat{\boldsymbol{r}}\cdot\boldsymbol{d}} \nabla_\Omega (F_\theta^* \mathrm{e}^{-\mathrm{j}k\hat{\boldsymbol{r}}\cdot\boldsymbol{d}}) \\ &= F_\theta \nabla_\Omega (F_\theta^*) - F_\theta F_\theta^* \mathrm{j}k \nabla_\Omega (\hat{\boldsymbol{r}} \cdot \boldsymbol{d}) \\ &= F_\theta \nabla_\Omega (F_\theta^*) - F_\theta F_\theta^* \mathrm{j}k (\nabla_\Omega \hat{\boldsymbol{r}}) \cdot \boldsymbol{d} \\ &= F_\theta \nabla_\Omega (F_\theta^*) - F_\theta F_\theta^* \mathrm{j}k (\hat{\boldsymbol{\theta}}\hat{\boldsymbol{\theta}} + \hat{\boldsymbol{\phi}}\hat{\boldsymbol{\phi}}) \cdot \boldsymbol{d}, \end{aligned} \tag{12}$$

and similarly for the ϕ component. Here,

$$\nabla_\Omega \hat{\boldsymbol{r}} = \hat{\boldsymbol{\theta}}\hat{\boldsymbol{\theta}} + \hat{\boldsymbol{\phi}}\hat{\boldsymbol{\phi}}$$

is used [4]. Note also that $\mathbf{A}_2$ and $F_\theta F_\phi^*$ are invariant under translations. By plugging (7) into (9), and using (12), it follows that

$$\begin{aligned} \boldsymbol{a}_1(\boldsymbol{F}') &= \boldsymbol{a}_1(\boldsymbol{F}) - k\left[\iint_\Omega \boldsymbol{F}^* \cdot \boldsymbol{F}(\hat{\boldsymbol{\theta}}\hat{\boldsymbol{\theta}} + \hat{\boldsymbol{\phi}}\hat{\boldsymbol{\phi}})\mathrm{d}\Omega\right] \cdot \boldsymbol{d} \\ &= -k\mathbf{A}_2 \cdot \boldsymbol{d}_{\text{RC}} - k\mathbf{A}_2 \cdot \boldsymbol{d} = -k\mathbf{A}_2 \cdot (\boldsymbol{d}_{\text{RC}} + \boldsymbol{d}). \end{aligned}$$

Hence, by (11) the new radiation center $\boldsymbol{d}'_{\text{RC}} = \boldsymbol{d}_{\text{RC}} + \boldsymbol{d}$ as expected.

IV. Results based on measured patterns

An algorithm employing the mode amplitudes $a_{\tau lm}$ of the SWE together with efficient Fast Fourier transform (FFT) based translation and rotation algorithms, have been used to calculate the radiation center $\boldsymbol{d}_{\mathrm{RC}}$, and the current distribution axis $\hat{\boldsymbol{r}}_{CD}$.

The first step of the algorithm is to find $\boldsymbol{d}_{\mathrm{RC}}$ by minimizing $L^2(\boldsymbol{d})$. In this step L^2 is calculated for seven translations using (4), and the coefficients of $L^2(\boldsymbol{d})$ are calculated by using (8). Thereafter, the minimum is found by using (11).

In a second step, the far field is translated to $\boldsymbol{d}_{\mathrm{min}}$, see Fig. 1. Thereafter, the current distribution axis is found by minimizing L_z^2 with respect to arbitrary rotations. In all cases reported here, a unique minimum was found.

The axial ratio of the current distribution is defined as

$$\mathrm{AR} = \sqrt{\min L^2 / \min L_z^2},$$

which is used in the plots to indicate the current distributions axes. The geometrical objects shown in the figures have been constructed from drawings of the antennas, and in some cases from direct length measurements.

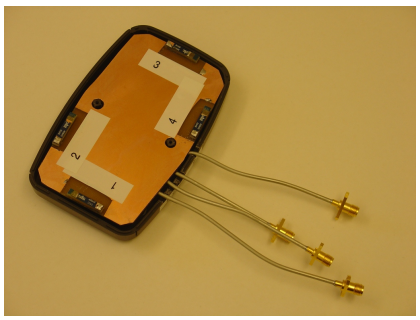

Fig. 2. Photo of a cellular phone mock-up with four antennas.

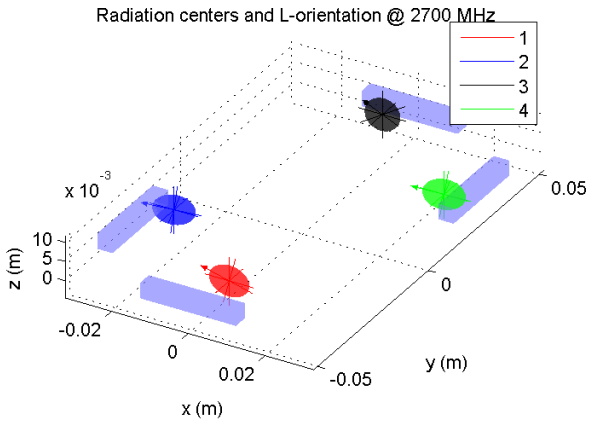

Fig. 3. Radiation centers and current distributions axes for four antennas on a cellular phone. The axial ratio of the ellipses indicate the ellipticity of the current distribution. The rather small axial ratio (AR) of the current distributions is typical for electrically small antennas.

A. Antennas on a cellular phone

In a first example antennas on a cellular phone are investigated, see Fig 2. Embedded far field patterns were measured in an unechoic chamber. The radiations centers are located slightly inside the antennas on the ground plane, see Fig 3. This indicates that the antenna currents flow partly on the antennas and partly on the ground plane.

B. Antennas on a laptop

In a second example, a laptop mock-up with four antennas on the lid is considered, see Fig. 4. These antennas were designed for low correlation and broad band operation. The measured far field data was used as input to the algorithm, and the radiation center and the current distribution axis were calculated for all ports at 750 MHz frequency. For the first three antennas, the radiation centers are in the plane of the lid, whereas for the rightmost antenna the radiation center is located slightly off the lid. The explanation for this could be radiation from the connecting cables or a measurement impairment such as turn table blocking, or reflections in the laptop keyboard. Note also the almost perpendicular current distributions for the two top antennas, designed for low correlation.

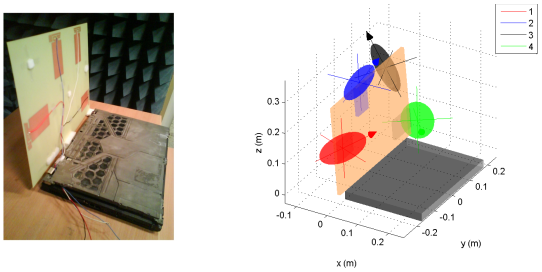

Fig. 4. Photo of the laptop computer equipped with four antennas (left) and radiation centers with current distributions axes (right).

C. Columns of a base station antenna

A base station antenna consists of four horizontally distributed columns each equipped with doubly polarized elements with 45 degree slanted co-polarizations, see Fig. 5. This antenna was purchased and investigated for beam forming and MIMO capacity. The zig-zag pattern between the radiation centers of the antenna columns, see Fig. 6, were later confirmed by dis-mounting the antenna radome.

As expected, a large axial ratio (AR) is found for the elongated antenna columns, see Fig 6. Note that the current distribution for each port consists of the total current on all antenna elements in a vertical antenna column. Another interesting note is that the axial ratio is slightly lower for the outer columns.

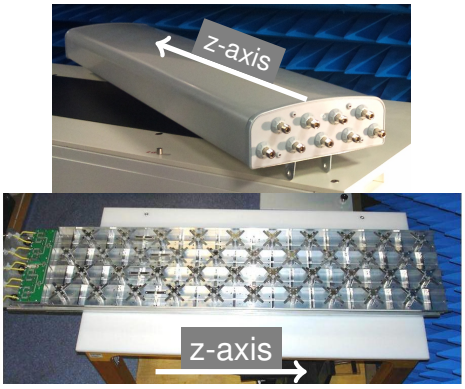

Fig. 5. A base station antenna with radome (upper) and without radome (lower), Courtesy of Tongyu Communication Inc. The antenna is equipped with eight antenna ports for the four columns of dual polarized antenna elements. The ninth port is used for electrical tilt control. In the lower photo it can be seen that the neighboring columns are shifted in a zig-zag pattern.

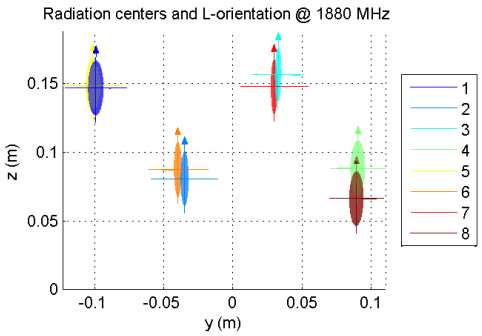

Fig. 6. Radiation centers and current distributions axes for the eight antenna ports of the base station antenna. For each antenna port, a column of 10 antenna elements, of either $+45^\circ$ or -45° slanted linear polarization, are fed.

D. Elements of a cylindrical array antenna

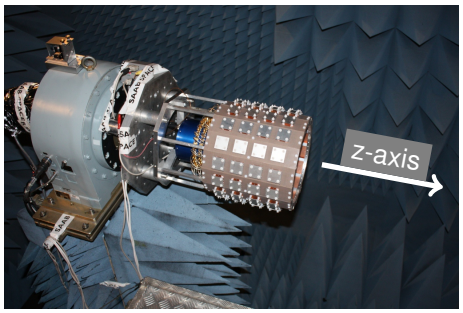

Fig. 7. Photo of the cylindrical array antenna, with 64 dual-polarized antenna patch elements on a faceted ground plane, mounted on the turn table ina roll over azimuth setup. A top view of the antenna, in its orientation of operation, is indicated with an arrow.

In a final example, we show a 64 element cylindrical array antenna with dual polarized vertical/horizontal elements, and designed for the band 2.5-2.6 GHz. The antenna element is a dual stacked patch, and the element separation is 58 mm, *i.e.*, $\lambda/2$ mm at 2.6 GHz, both in the vertical and the horizontal direction. Embedded far field patterns at 2.5 GHz for all the 128 antenna ports were used as input to the algorithm. The array antenna is depicted in Fig. 7. The radiation centers for both polarizations and all 64 elements are depicted in Figs 8a and b. Measurement impairments can be identified for at least two elements in the bottom row, *i.e.* the row closest to the turn table, see Fig. 8. The results for the vertical and horizontal antenna polarizations are quite similar. Therfore, only results for the vertical polarization are shown.

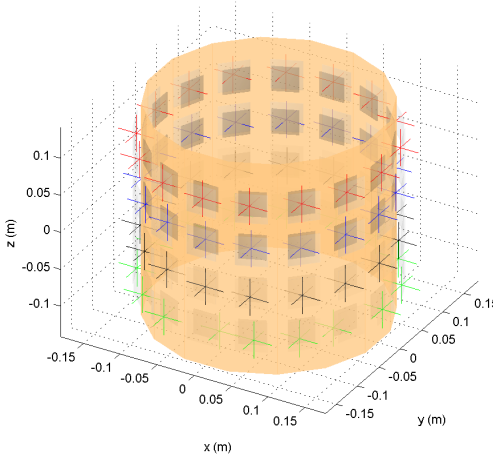

(a) 3D view

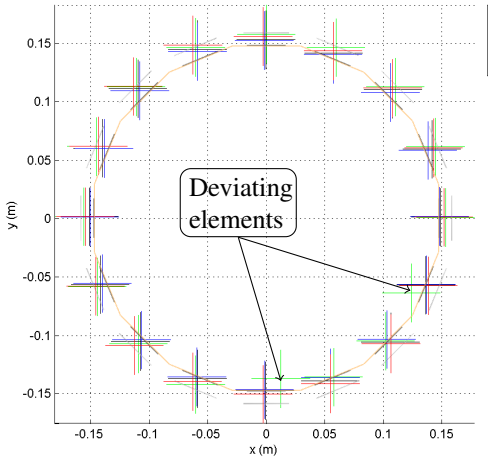

(b) Top view, see Fig. 7

Fig. 8. Radiation centers for the 64 element cylindrical array for the vertically polarized antenna ports. The radiation centers are depicted as three-dimensional crosses. A pair of stacked patches, for each antenna element, are depicted as gray squares. The outer patch is slightly larger than the inner. In the top view the antenna is viewed from the positive z-axis, see Fig. 7. For two elements in the bottom row the radiation centers deviate from the general trend which could be due to measurement impairments, *e.g.* reflections in the turn table, see Fig. 7.

V. Conclusion

The benefits of defining a radiation center using angular momentum compared to the standard definition of phase center [2] are: uniqueness is guaranteed; the numerical algorithm is robust and fast if only translations and rotations are efficiently implemented. Moreover, the method applies for any radiation pattern. In addition, the orientation, ellipticity, and electrical size of the antenna currents can be retrieved.

A numerical algorithm has been implemented and tested on measured far field pattern data for a number of different antenna types. The results show good agreement with mechanical drawings of the antennas. Deviations from the mechanical positions have reasonable explanations, *e.g.* currents on the ground plane or measurement impairments. This method can be used to detect the position of the antenna currents and to detect measurement impairments. The exact physical meaning of the radiation center is a task of future work.

References

[1] J. Hald, J. E. Hansen, F. Jensen, and F. Holm Larsen, *Spherical Near-Field Antenna Measurements*, ser. IEE electromagnetic waves series, J. Hansen, Ed. Peter Peregrinus Ltd., 1998, vol. 26, edited by J.E. Hansen.

[2] *IEEE145-1993. IEEE Standard Definition of Terms for Antennas*, Antenna Standards Committee of the IEEE Antennas and Propagation Society Std., Mar. 1993.

[3] J. Fridén and G. Kristensson, "Calculation of antenna radiation center using angular momentum," Lund University, Department of Electrical and Information Technology, P.O. Box 118, S-221 00 Lund, Sweden, Tech. Rep. LUTEDX/(TEAT-7219)/1–23/(2012), 2012, http://www.eit.lth.se.

[4] J. G. Van Bladel, *Electromagnetic Fields*, 2nd ed. IEEE Press, 2007.